IEEE Sensors Letters Volume 2(3) (2017)
Article Subject (see Index Terms below and write one here)

Design of a Novel Optical Overhead Line Monitoring Sensor

Jack Marston[1], Grzegorz Fusiek[1*], and Pawel Niewczas[1*]
[1] *Department of Electronic and Electrical Engineering, University of Strathclyde, Glasgow, United Kingdom*
**Member, IEEE*

Received 25 Apr 2024, revised 5 May 2024, accepted 30 May 2024, published 5 Jun 2024, current version 15 Dec 2024. (Dates will be inserted by IEEE; "published" is the date the accepted preprint is posted on IEEE Xplore®; "current version" is the date the typeset version is posted on Xplore®).

Abstract—This letter reports on the design of a novel optical overhead line (OHL) monitoring sensor for determining key mechanical line parameters in electrical power networks. The sensor employs fiber Bragg gratings (FBGs) that are inscribed in a metal-coated fiber and encapsulated in a Kovar® capillary. The epoxy-free construction of the sensor ensures high-performance hermetic sealing of the FBGs making the proposed sag sensor suitable for monitoring standard low-temperature as well as high-temperature low-sag (HTLS) overhead line conductors. The sensor construction allows for direct measurements of the conductor strain and temperature of up to ±2000 µm/m (µstrain) and up to 450 °C, respectively, and indirect measurements of sag and other parameters such as tension force and stress in the conductor. The sensor design optimization is performed by means of the finite element analysis (FEA), allowing the expected strain transfer from the conductor to the strain sensor to be investigated theoretically. It is demonstrated that the proposed design of the sensor, with a simulated strain transfer of 52%, is suitable for providing sag measurements within the required ranges. The proposed sensor has the potential for multiplexing on a single optical fiber and thus can be used for the determination of OHL sag, temperature, and vibration over a wide-area power network, enabling precise dynamic line rating and condition monitoring functions.

Index Terms— Fiber Bragg gratings, optical sag sensor, overhead line conductors, power grids, FEA design optimization

I. INTRODUCTION

The electricity transmission and distribution power networks utilize overhead lines (OHLs), underground cables (UCs), transformers, and other equipment to supply energy to end users. The growth in electricity consumption observed in recent years, combined with the expanding penetration of renewables with weather-dependent variable power output, requires the existing transmission lines' capacity to be increased [1], [2].

To increase the peak throughput, efficiency and reliability of the electrical grid, dynamic line rating (DLR) systems have been developed [1], [2]. These systems rely on atmospheric climatic conditions and the overhead line parameters including sag and temperature to determine the temporal current carrying capacity of the line [3], [4]. Apart from the DRL systems, various line types including hard-drawn copper or aluminum conductors or special high-temperature low-sag (HTLS) conductors with operating temperatures up to 180 °C, and short-time operation up to 250 °C have been employed to enhance the grid capacity [4].

However, to benefit from the DLR technology, the condition monitoring of the OHL conductors, either by using a combination of weather data from meteorological models and local sensors to estimate the actual status of the line and its capacity, or by direct measurements of the physical parameters of the lines including temperature, sag, tension, and vibrations is required [5].

Several different conventional technologies have been used for OHL parameters monitoring including current, temperature, sag, humidity, illumination, bending, or vibration which were realized using electronic, optoelectronic, or optical sensors [6]–[11]. Some of the proposed solutions are not suitable for adverse temperature conditions or long-distance coverage, such as, e.g., wireless electronic sensors, the use of which is also limited by network operators due to cybersecurity concerns. A comparison between various sag sensors' performance, their benefits, and drawbacks are discussed in [11].

As part of a holistic measurement system allowing for monitoring both electrical and mechanical OHL parameters, sag, temperature, and vibration sensors employing the fiber Bragg grating (FBG) technology, and being compatible with other optical FBG-based voltage and current sensors, were previously proposed by the authors [4], [12]–[14]. The previous sag sensor designs consisted of the FBG-based strain and temperature sensors spatially separated from the conductor by a distance of 5 mm [14], which could cause the temperature measured by the sag sensor to deviate from the temperature of the conductor, accentuated for strong winds.

In this paper, an improved design of an optical sag sensor is proposed. The strain and temperature sensors are meant to be spot-welded to an SS304 mounting sleeve encompassing the monitored conductor to ensure an improved thermal contact of the FBGs with the conductor. By bringing the strain and temperature sensors closer to the conductor surface, more accurate conductor temperature measurement can be performed which is the major improvement and benefit of the new sensor design. Moreover, the design is epoxy-free, eliminating any moisture- or temperature-induced mechanical

Corresponding author: G. Fusiek (g.fusiek@strath.ac.uk).
Digital Object Identifier: 10.1109/LSEN.XXXX.XXXXXXX (inserted by IEEE).

coupling changes between the substrate and the FBG.

Consequently, this paper concentrates on the design and theoretical evaluation of the optical sag sensor for monitoring overhead line conductors. The sensor is equipped with a strain sensor and a temperature sensor to provide both an independent absolute temperature sensor and a precise temperature compensator. The paper provides the details of sensor construction and the optimization of the design by employing finite element analysis (FEA) to ensure adequate strain transfer from the conductor to the strain sensing FBG.

II. SAG SENSOR SPECIFICATIONS

A. Design requirements

The OHL monitoring sensor was specifically designed for installation on a hard-drawn copper (HDC) conductor with a cross-section of 70 mm^2 available on an OHL at the Power Network Demonstration Centre (PNDC) at the University of Strathclyde, UK [15]. The HDC conductor has 7-strands and a diameter of 10.5 mm. The distance between the poles of the line, measured with a distance meter, was 88 m. The tension force in the conductor was 3.45 kN at the ambient temperature of 10 °C when measured with a dynamometer. The maximum operating temperature limit of the conductor is assumed to be 75 °C [15].

The conductor sag can be related to the measured strain in the conductor by the following equation [14]:

$$D = \sqrt{[3S(L_c(1+\varepsilon) - S)]/8} \qquad (1)$$

where D is the conductor sag, S is the span of the line (distance between two poles), L_c is the initial conductor length and ε is the strain measured by the sensor equal to the change in the distance between the clamps (a relative elongation of L_c). To allow for calculations of the absolute sag and clearance to the ground, the initial horizontal tension in the conductor, as well as its initial sag and length at the conductor installation, must be known [14].

The operational conditions of the considered conductor were assumed to be within temperatures of -20 °C to 75 °C, with the conductor tension between 2.3 kN to 14.5 kN for winds up to 35 m/s, resulting in a measured strain range of ±2000 μstrain [14].

B. Optical Strain and Temperature Sensors

The proposed sag sensor is equipped with two FBG-based sensors for measuring strain and temperature in the monitored conductor. Each sensor utilizes a 10-mm long FBG inscribed in a 15-mm long bare section of a copper-coated fiber [16], and is encapsulated in a Kovar® capillary by brazing the components together with a silver-based paste at around 620 °C using an induction heating system [17], [18]. The construction of the strain and temperature sensors was adopted from the previous design by the authors [19], with a capillary length of 35 mm, and inner diameter (ID) and outer diameter (OD) of 200 μm and 700 μm, respectively.

The strain sensor is equipped with two stainless steel 304 (SS304) 0.2-mm thick and 10-mm long shims to which both ends of the capillary are brazed [18], [19]. In the proposed design, the temperature sensor is brazed at only one end to one of the strain sensor shims, as shown in Fig. 1. Thus, it is decoupled mechanically from strain and serves as both an independent absolute temperature sensor and a precise temperature compensator. This is required as FBGs are sensitive to strain and temperature [20].

The construction of the strain and temperature sensors ensures that strain and temperature measurements can be performed simultaneously by the sag sensor and the sensors are suitable for high-temperature operation up to 450 °C (long-term) [16]–[18]. This packaging method eliminates the use of epoxy for sensor attachment and the influence of moisture on the sensor performance, as well as provides an armor around each FBG to protect it from damage, making the solution well suited to harsh industrial environments.

C. Sag Sensor Construction

The illustrative diagram of the proposed sag sensor construction and its installation on a conductor is shown in Fig. 1.

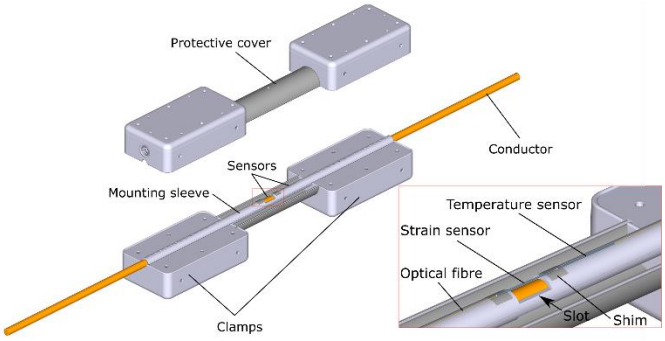

Fig. 1. Optical sag sensor mounted on the HDC conductor.

Due to the safety requirements, the attachment of the sensors must ensure that there is no direct interference in the conductor structure. Therefore, to construct the sag sensor, the strain and temperature sensors are designed to be spot-welded to an SS304 mounting sleeve that will encompass the conductor to ensure an improved thermal contact of the FBGs with the conductor. Note that the previous sensor iteration consisted of the FBG sensors spatially separated from the conductor by a distance of 5 mm [14], which could cause the temperature measured by the sag sensor to deviate from the temperature of the conductor, particularly accentuated for strong winds. By bringing the strain and temperature sensors closer to the conductor surface, more accurate conductor temperature measurement can be performed which is the major improvement and benefit of the proposed sensor design.

As can be seen from Fig. 1, the OHL sensor is assembled using the top and bottom parts to allow for its installation on the conductor. Each half of the mounting sleeve is fixed to the clamps with M1 countersunk screws. The clamp region consists of three parts: a top plate, a middle plate, and a bottom plate. The bottom plate has six M5 threads (and the two top plates have corresponding through holes) that are used to clamp the sensor onto the conductor using bolts.

The protective cover (see Fig. 1) with ID/OD 35/42 mm has a hole to allow for the injection of a potting gel after the installation on the conductor. This is to prevent water ingress into the enclosure. The potting gel used needs to be sufficiently soft to not affect the strain sensor response. The top clamps of the sag sensor have small grooves

and compartments for fiber management and regions to interface with the external optical cable (not shown in Fig. 1).

To reduce the stiffness and increase the strain transfer from the conductor to the strain sensor, a slot (material cut-out) has been added to the mounting sleeve underneath the strain sensor, as can be seen in Fig. 1. The slot has been added symmetrically on the other half of the sleeve to prevent bending under tension. Since the size of the slot affects the strain transfer between the conductor and the strain sensing FBG, the sag sensor design was optimized using finite element analysis (FEA) and the Solid Mechanics module in COMSOL Multiphysics® software as described in the next section.

III. SENSOR DESIGN OPTIMIZATION

A. Finite Element Analysis Settings

Finite element analysis was carried out for a range of dimensions of the mounting sleeve and the slot for which the strain in the FBG section was compared to that in the conductor.

The geometries of the conductor and the mounting sleeve with the strain sensor attached across the slot were imported to COMSOL, as shown in Fig. 2.

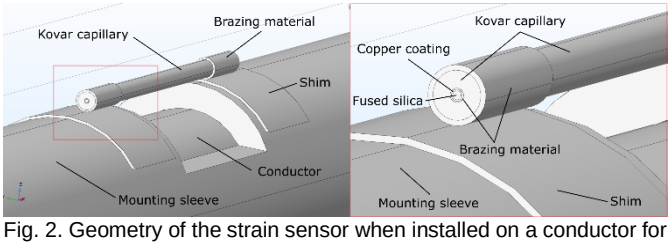

Fig. 2. Geometry of the strain sensor when installed on a conductor for FEA purposes.

To simplify the finite element analysis, the HDC conductor was modeled as a solid rod with a diameter of 10.5 mm. The length of the brazed joints between the Kovar capillary and the copper coating of the fiber was assumed to be 2 mm long with a thickness of 17.5 µm, consistent with our experiments of the visualization of the sample joints through polishing (not shown here). The brazing material was assumed to be 55% silver solder. The solder material thickness between the capillary and the shim was set to 0.3 mm over a 6-mm length.

The selected mechanical properties of the materials used for FEA are summarized in Table 1.

Table 1. Selected mechanical properties of the materials used for FEA.

Material	Young's Modulus, E (GPa)	Poisson's Ratio, ν	Coefficient of Thermal Expansion, CTE (ppm/K)
Fused Silica	73	0.17	0.48
Copper Coating	135	0.35	17
Conductor	120	0.35	17
Brazing Material	83	0.36	19.5
Kovar	138	0.317	5
SS304	193	0.30	17.3

In the considered finite element model (FEM), the mounting sleeve is only attached to the conductor in the clamp region (160 mm) with a roller constraint applied in the sensor region between the clamps (162 mm) to allow it to slide freely over the conductor surface. This simulates the sensor being clamped onto the conductor at the ends. A boundary axial load was applied to one end of the copper conductor of 3.45 kN while the other end was fixed.

A series of simulations were performed in COMSOL using a static study with a parametric sweep of the dimensions of the mounting sleeve and the slot at a temperature of 20 °C. The thickness of the sleeve as well as the length and the depth of the slot varied within specified ranges. The strain measured by the strain sensor was estimated along the fiber surface. The ratio of the strain measured by the strain sensor and the strain in the conductor outside the sag sensor was taken to find the strain transfer of the sensor as a percentage. The results of this investigation are presented below.

B. Results

An example of the strain distribution in the conductor and the strain sensor fiber for a mounting sleeve thickness of 2 mm, a slot depth of 4 mm, and a slot length of 20 mm is shown in Fig. 3 and Fig. 4. The strain in the fiber is around 165 µstrain while the strain in the conductor outside the clamps (not shown in Fig. 3) is nearly 320 µstrain resulting in a strain transfer of 52%.

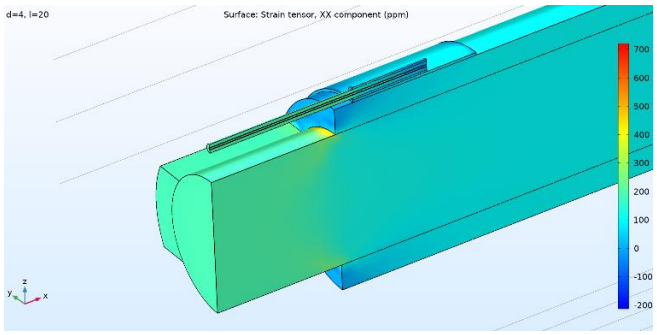

Fig. 3. Strain distribution in the conductor and the strain sensor (a quarter of the geometry is shown).

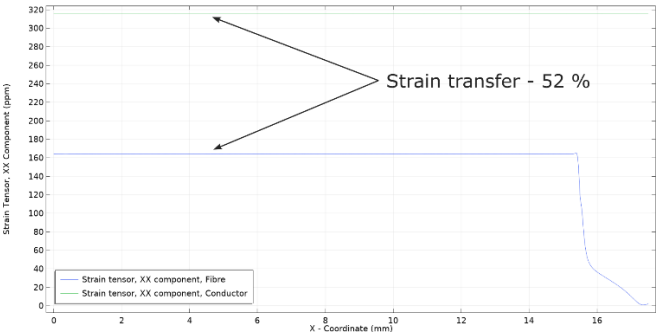

Fig. 4. Comparison of the strain detected by the strain sensor along the fiber and the conductor outside the sag sensor clamps.

The results of the parametric sweep for a range of the dimensions of the mounting sleeve and the slot are shown in Fig. 5 and Fig. 6. As can be seen from Fig. 5, strain transfer is inversely proportional to sleeve thickness, with a maximum strain transfer of approximately 65% at a slot depth of 4 mm and length of 20 mm, and sleeve thickness of 1 mm. However, at 1 mm sleeve thickness, it was decided that the likelihood of damage during installation or construction was high. Therefore, a sleeve thickness of 2 mm was selected as an optimum to maximize the strain transfer while preventing its damage.

The strain transfer dependence on the slot size at a mounting sleeve thickness of 2 mm can be observed in Fig. 6. Clearly, longer slots at their greater depth allow to achieve greater strain transfers.

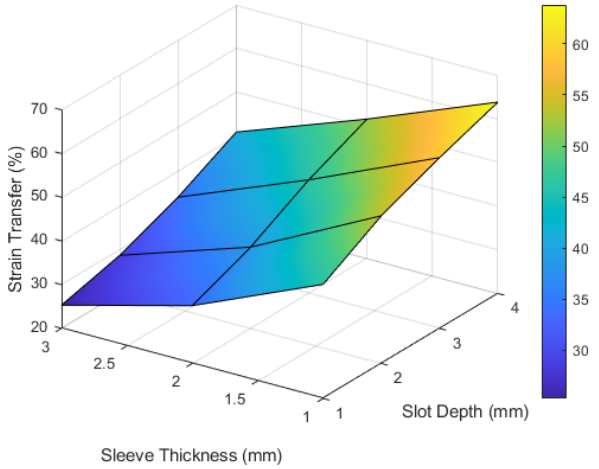

Fig. 5. Strain transfer from the conductor to the strain sensor as a function of sleeve thickness and slot depth at the 20-mm slot length.

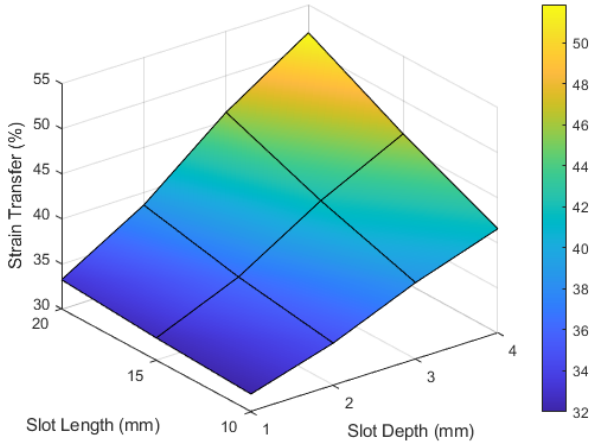

Fig. 6. Strain transfer from the conductor to the strain sensor as a function of the slot depth and length at the 2-mm sleeve thickness.

Consequently, the mounting sleeve thickness of 2 mm and the slot depth of 4 mm at the length of 20 mm (limited by the length of the Kovar capillary and FBG) were selected as optimal for the final design of the sag sensor.

IV. CONCLUSION

In this paper, the design of a novel optical sag sensor employing FBG-based strain and temperature sensors has been presented. The design optimization was carried out using FEA to ensure adequate strain transfer from the conductor to the strain sensor. It was demonstrated that the strain transfer of 52 % from the conductor to the strain sensor can be readily achieved. The FEA results show that the sag sensor should be suitable for monitoring the mechanical parameters of the OHL conductors within the required operating range. Future work will focus on the FEA of the sensor's thermal performance followed by the fabrication and laboratory characterization of the designed sag sensor.

ACKNOWLEDGMENT

The research presented in this letter was carried out within the PHOENIX project funded by The Energy Entrepreneurs Fund - Phase 9 within the Department for Business, Energy, and Industrial Strategy (BEIS), UK. All data underpinning this publication are openly available from the University of Strathclyde Knowledge Base at https://doi.org/10.15129/8cf1901e-9df2-48c9-bb69-feefdd7543a3.

REFERENCES

[1] S. Karimi, P. Musilek, and A. M. Knight, "Dynamic thermal rating of transmission lines: A review," *Renew. Sustain. Energy Rev.*, vol. 91, pp. 600–612, 2018, doi: https://doi.org/10.1016/j.rser.2018.04.001.

[2] Y. Hou *et al.*, "Research and application of dynamic line rating technology," *Energy Reports*, vol. 6, pp. 716–730, 2020, doi: https://doi.org/10.1016/j.egyr.2020.11.140.

[3] E. Fernandez, I. Albizu, M. T. Bedialauneta, A. J. Mazon, and P. T. Leite, "Review of dynamic line rating systems for wind power integration," *Renew. Sustain. Energy Rev.*, vol. 53, pp. 80–92, 2016, doi: 10.1016/j.rser.2015.07.149.

[4] H. Singh, G. Fusiek, and P. Niewczas, "Extended characterization of an optical sag sensor for high-temperature low-sag lines," *IEEE Sensors Lett.*, 2023.

[5] CIGRE TF B2.11.07, *Technical Brochure 332: Fatigue Endurance Capability of Conductor / Clamp Systems - Update of Present Knowledge*, no. October. 2007.

[6] F. V. B. de Nazare and M. M. Werneck, "Hybrid Optoelectronic Sensor for Current and Temperature Monitoring in Overhead Transmission Lines," *IEEE Sens. J.*, vol. 12, no. 5, pp. 1193–1194, 2012, doi: 10.1109/JSEN.2011.2163709.

[7] H. Wang, S. Han, L.-J. Lv, and L.-J. Jin, "Transmission line sag measurement based on single aerial image," in *2017 24th International Conference on Mechatronics and Machine Vision in Practice (M2VIP)*, IEEE, 2017, pp. 1–5. doi: 10.1109/M2VIP.2017.8211435.

[8] M. Wydra, P. Kisala, D. Harasim, and P. Kacejko, "Overhead transmission line sag estimation using a simple optomechanical system with chirped fiber bragg gratings. part 1: Preliminary measurements," *Sensors (Switzerland)*, vol. 18, no. 1, 2018, doi: 10.3390/s18010309.

[9] T. S. Hsu *et al.*, "An IoT-based Sag Monitoring System for Overhead Transmission Lines," in *2019 IEEE PES GTD Grand International Conference and Exposition Asia (GTD Asia)*, IEEE, 2019, pp. 515–519. doi: 10.1109/GTDAsia.2019.8715975.

[10] K. Kopsidas, S. A. Rahman, M. A. AlAqil, and S. Rolfo, "Advancing OHL Rating Calculations: Modeling Mixed-Convective Cooling and Conductor Geometry," *IEEE Trans. Power Deliv.*, vol. 38, no. 1, pp. 610–619, 2023, doi: 10.1109/TPWRD.2022.3197325.

[11] X. D. Yunfei Chen, "A survey of sag monitoring methods for power grid transmission lines.," *IET Gener. Transm. \& Distrib.*, 2023.

[12] H. Singh, G. Fusiek, P. Niewczas, and V. Livina, "Estimation of the Fatigue Life of a Fiber Bragg Grating Overhead Line Sag Sensor," in *I2MTC 2024 - 2024 IEEE International Instrumentation and Measurement Technology Conference, Proceedings*, 2024.

[13] G. Fusiek, H. Singh, and P. Niewczas, "Temperature and force characterization of an optical sag sensor for overhead line monitoring," in *2023 IEEE International Instrumentation and Measurement Technology Conference (I2MTC)*, 2023.

[14] G. Fusiek and P. Niewczas, "Design of an optical sensor with varied sensitivities for overhead line sag, temperature and vibration monitoring," in *2022 IEEE International Instrumentation and Measurement Technology Conference (I2MTC)*, IEEE, 2022, pp. 1–6. doi: 10.1109/I2MTC48687.2022.9806489.

[15] H. Singh, G. Fusiek, P. Niewczas, and V. Livina, "Estimation of the Fatigue Life of a Fiber Bragg Grating Overhead Line Sag Sensor," in *I2MTC 2024 - 2024 IEEE International Instrumentation and Measurement Technology Conference, Proceedings*, [in press].

[16] IVG Fiber, "Copper-coated single mode fiber, Cu1300." Accessed: Apr. 17, 2024. [Online]. Available: https://www.ivgfiber.com/datasheet_singlemode.pdf

[17] P. Niewczas and G. Fusiek, "Induction heating assisted optical fiber bonding and sealing technique," in *Proceedings of SPIE - The International Society for Optical Engineering*, 2011. doi: 10.1117/12.885942.

[18] G. Fusiek, P. Niewczas, and M. Johnston, "Metal-packaged Fiber Bragg Gratings for Structural Health Monitoring," in *Optics InfoBase Conference Papers*, 2014.

[19] J. McAlorum, G. Fusiek, T. Rubert, and P. Niewczas, "Concrete fatigue experiment for sensor prototyping and validation of industrial SHM trials," in *2019 IEEE International Instrumentation and Measurement Technology Conference (I2MTC)*, IEEE, May 2019, pp. 1–6. doi: 10.1109/I2MTC.2019.8827036.

[20] Y.-J. Rao, "In-fibre Bragg grating sensors," *Meas. Sci. Technol.*, vol. 8, no. 4, pp. 355–375, Apr. 1997, doi: 10.1088/0957-0233/8/4/002.